



ORIGINAL ARTICLE

Physicochemical assessment of prednisone adsorption on two molecular composites using statistical physics formalism in cosmetics

Sarra Wjihi^a, Fatma Aouaini^{a,b,*}, Aljawhara H. Almuqrin^b,
Abdelmottaleb Ben Lamine^a

^a Laboratory of Quantum and Statistical Physics, LR18ES18, Faculty of Sciences of Monastir, Tunisia

^b Physics Department, Faculty of Science, Princess Nourah Bint Abdulrahman University, Riyadh, Saudi Arabia

Received 29 April 2020; accepted 30 June 2020

Available online 9 July 2020

KEYWORDS

Adsorption isotherm;
Prednisone in cosmetics;
Modeling analysis;
Thermodynamics potentials

Abstract In this paper, we consider two different polyethylene filter plates coated with multi-walled carbon nanotubes (MWCNTs) and synthesized by surface molecularly imprinted technique, namely plate@MWCNTs@MIPs (PMIPs) and plate@MWCNTs@NIPs (PNIPs). They were used as effective adsorbents for selective adsorption and detection of prednisone (PS) in cosmetics. As a first assessment to investigate the performance of these adsorbents, the PS adsorption isotherms were analyzed using an advanced multilayer statistical physics model at three different temperatures (293, 303 and 313 K) and over a wide PS concentration range (0.09–1.5 mg/mL). The obtained analyzing results from the best fitting model showed that the PMIPs adsorbent displayed a high adsorption capacity (27.4 mg/g) due to the contribution of the number of PS molecules per site (n_m) combined with the receptor sites density (D_m), which displayed a high recognition ability due to the adsorption energy. Modeling analysis process indicated that the PS molecules could be anchored on the PMIPs and PNIPs surfaces via a non-parallel orientation where the adsorption is a multi-molecular process. The calculated adsorption energies globally varied from 4.51 to 7.62 kJ/mol, confirming the physical nature of the adsorption process for the studied systems, which is beneficial in cosmetics. Finally, three thermodynamic potentials (entropy, internal energy and free enthalpy) were evaluated for a better understanding of the physico-chemical behavior of the adsorption process.

© 2020 Published by Elsevier B.V. on behalf of King Saud University. This is an open access article under the CC BY-NC-ND license (<http://creativecommons.org/licenses/by-nc-nd/4.0/>).

* Corresponding author at: Laboratory of Quantum and Statistical Physics, LR18ES18, Faculty of Sciences of Monastir, Tunisia.

E-mail addresses: sarawjihi@yahoo.fr (S. Wjihi), fatmasaidi965@gmail.com (F. Aouaini).

Peer review under responsibility of King Saud University.



Production and hosting by Elsevier

1. Introduction

Prednisone is a glucocorticoid (GCs) mainly employed in the treatment of dermatological diseases and many other diseases (Li et al., 2013). The application of prednisone in cosmetics leads to an enhancement in the smoothness and texture of the skin. Nevertheless, prolonged use of these hormone-based cosmetics may lead to hormonal addiction in relation with other side effects, which can cause metabolic disorders or even cancer (Capelli et al., 2013; Fiori and Andrisano, 2014.LC-MS; Zhang et al., 2016). Thus, The European Union Cosmetics Regulation (Santoni, 2015) forbids the use of glucocorticoids in cosmetics. However, some illegal manufacturers have been found to add anti-inflammatory GCs to their cosmetics to achieve anti-acne and anti-wrinkle effects (Gagliardi et al., 2000; Gagliardi et al., 2002; Reepmeyer et al., 1998). Consequently, there is a great demand to develop an advanced technique capable of detecting the adulteration of GCs in cosmetics. Currently, many techniques such as liquid chromatography (HPLC) (Fu et al., 2010), capillary electrophoresis (Bagot and Meaney, 2011), thin layer chromatography (Rodionova et al., 2010) and gas chromatography (GC)-mass spectrometry (MS) (Antignac et al., 2004) have been used in order to recognize and examine forbidden ingredients in cosmetic products. However, these techniques are often time consuming, complicated and require considerable amounts of reagents and solvents. Hence, choosing a suitable preparation technique is essential for the efficient examination of complex samples. Solid phase extraction with a surface molecular imprint (SMISPE) is a significant method for sample elaboration. This technique has better selectivity for prohibited substances, and is simple to prepare compared to conventional separation methods (Anderson et al., 2008; Arabi et al., 2020; Bianchi et al., 2017). Additionally, prednisone molecular capture (PS-MC) is a new SMISPE substrate, and is prepared using surface molecular imprinting technology (Gong et al., 2018; Kamra et al., 2015; Liu et al., 2015; Liu et al., 2017; Nematollahzadeh et al., 2014; Wei et al., 2015) with multi-walled carbon nanotubes (MWCNTs) (Ertan et al., 2016; Kumar et al., 2014; Luo et al., 2012; Zhang and Shi, 2012; Zhang et al., 2010; Zhao et al., 2016). PS-MC has many characteristics of molecularly imprinted polymers (MIPs), such as excellent separation and adsorption selectivity for guest molecules. In addition, PS-MC has the characteristics of solid phase extraction separation (Akram and Dorabei, 2017; Zong-Yuan et al., 2014); after having completed the recognition and adsorption of the template molecules (prednisone), it can be eliminated immediately from the sample matrix without the need for a high speed centrifugation or magnetic separation. The PS-MC used in this study was prepared through the surface polymerization combined with nanotechnology (Wang et al., 2018). A plate@MWCNTs was employed as an inner backing and then covered with molecularly imprinted polymers (MIPs) using the entrapping technique. The MIPs were coated on the plate@MWCNTs surface via the copolymerization of a functional monomer (APTES), a cross-linking agent (TEOS), and the template molecules (prednisone). Finally, the template molecules were eliminated to yield the PS-MC (Wang et al., 2018). Studying the adsorption equilibrium is essential to understand the binding properties of PS-MC to prednisone (Almughamisi et al., 2020; Elwakeel et al., 2020; Zhou et al.,

2020). The adsorption of prednisone and other similar molecules on various adsorbent compounds have been analyzed through empirical sorption models (Toth, Langmuir, Freundlich, etc.), thanks to their simplicity and flexibility (Bouaziz et al., 2019; Song et al., 2017; Song et al., 2017; Wang et al., 2018; Zhang et al., 2019). However these classical models generally provide an incomplete understanding of the sorption process, due to the strong restrictions of their fundamental assumptions. In this paper, the prednisone sorption isotherms onto plate@MWCNTs@MIPs (PMIPs) and plate@MWCNTs@NIPs (PNIPs) adsorbents were theoretically investigated to better understand and interpret the adsorption process. The aim of the work is the assessment of a modelling analysis based on the statistical physics formalism as a new tool for the retrieving of important adsorption parameters with a defined physical meaning, i.e. the number of prednisone molecules captured per binding site of the adsorbent, the density of the receptor sites of the tested adsorbents, the total number of the formed layers of prednisone on the adsorbent surface, the surface adsorption energies, etc. In light of this clarification, the experimental tests only aim to build a significant and sufficiently large dataset to which the statistical physics models apply for the subsequent and most meaningful modelling analysis. Three advanced statistical physics models have been implemented in order to attribute new microscopic and macroscopic interpretations to prednisone molecule adsorption onto plate@MWCNTs@MIPs (PMIPs) and plate@MWCNTs@NIPs (PNIPs). Indeed, these theoretical models were applied for the first time for the interpretation of the prednisone adsorption and allowed a significant extension of the modelling power offered by the classical models (e.g. Langmuir, Hill and BET), commonly adopted in this field of investigation. The use of a new set of adsorption models derived from the statistical physics for the modelling analysis of prednisone adsorption onto PMIPs and PNIPs has never been proposed in the literature. Not only is the theoretical modelling aspect important, but the consequences of this modelling are also more relevant than the used statistical physics method.

The selection of the best fitting is itself data of the physicochemical information about the description and details of the adsorption process. It is like a microscope which shows and highlights the microscopic aspects of the adsorption process, such as the molecule position, molecule adsorption energy, the molecule stacking layer, specific area of the porous adsorbent structure, energy distribution, and energy distribution of the surface heterogeneity. These aspects are derived from the physical parameters of the selected model and investigated in this paper. Indeed, this best fitting model allows the calculation of several adsorption parameters with a defined physical meaning, which helps in the analysis of adsorption systems with a significantly deeper detail compared to the commonly adopted modelling analysis (e.g. those based on the Langmuir or Freundlich models).

Another goal is to accurately analyze the thermodynamics of the prednisone adsorption and to treat the effect of the main sorption parameters. This model is intended for a support tool for the adequate design of a novel solid phase extraction material with specific adsorption for prednisone. It also allows the selection of sorbent composites with microstructural and chemical characteristics suitable for the detection of prednisone in cosmetic products. The energy distribution of the site was also estimated to corroborate the surface heterogeneity

and the physical nature of the adsorbate/adsorbent interactions. This allows to characterize the linking energy of prednisone with organic materials. The physisorption character allows to ensure the reversibility of the PS anchorage to be able to remove the PS molecules from these composites from the human skin.

2. Experimental details

2.1. Materials

The preparation and characterization of the plate@MWCNTs@MIPs (PMIPs), and plate@MWCNTs@NIPs (PNIPs) can be referred to literature (Wang et al., 2018). The difference between the two modified adsorbents is that the PNIPs material is prepared according to the same methodology as PMIPs but without the introduction of a prednisone template (Wang et al., 2018). The molecular structure of this prednisone molecule is presented in Fig. 1.

2.2. Adsorption isotherms experiments

The Prednisone adsorption isotherms on PMIPs and PNIPs adsorbents were determined at temperatures 293 K, 303 K and 313 K according to the experimental conditions introduced in (Wang et al., 2018). In each experiment, four pieces of PMIPs and PNIPs were placed in a wide-mouth bottle and 10 mL of prednisone solution (1 mg/mL) was added. Then, the bottle was covered and incubated during 2.5 h. PS-MC that reached the adsorption equilibrium was separated from the prednisone solution. The UV-Vis spectrometry is used to determine the concentration of prednisone in the supernatant. All the experimental data of PS adsorption on PMIPs and PNIPs have been reported in (Wang et al., 2018), and they are illustrated in Fig. 2. The PS sorption isotherms demonstrated that the temperature had an impact on the evolution of the uptake quantity. This thermal impact on the adsorbents can be examined through the implementation of theoretical sorption models.

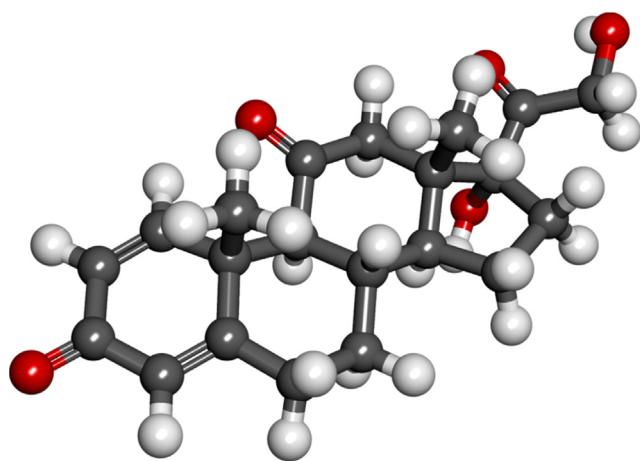


Fig. 1 3D representation of the molecular structure of the Prednisone. Colors: gray—carbons, white—hydrogen and red—oxygen.

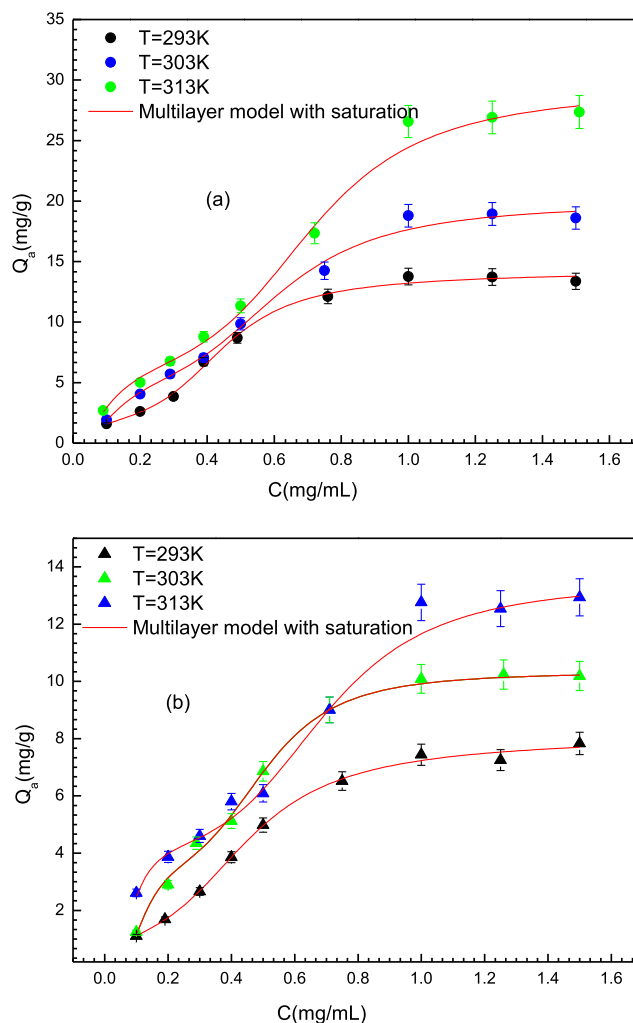


Fig. 2 Adsorption isotherms of PS on (a) PMIPs and (b) PNIPs at three different temperature (293–303–313 K) and over a concentration range of (0.09–1.5 mg/mL) fitted by multilayer statistical physics model (M3).

3. Description of prednisone sorption profiles and modeling analysis

Fig. 2a and 2b depict the PS sorption isotherms at 293 K, 303 K and 313 K on PMIPs and PNIPs adsorbents, respectively. The PS adsorption quantities reach a fixed value at a high concentration highlighting the typical saturation process. This process is the consequence of the site occupation with PS molecules by the creation of two or more layers. According to the PS isotherm behavior, three advanced models were established to mathematically interpret and discuss the prednisone sorption phenomenon from cosmetic products.

3.1. Sorption with the creation of single layer (M1)

This adsorption model assumed that the PS sorption was performed with a fixed number of layers (one layer in this state) with one binding energy ($-\epsilon$). In addition, we supposed that every binding site included in the sorption process captured a variable number of PS molecules. In fact, this statistical

model allows the captured number of PS per main adsorption site to be greater or less than unity. Hence, the variation of the uptake capacity is written by the following equation (Aouaini et al., 2019):

$$Q_a = \frac{n_m \cdot D_m}{\left(1 + \left(\frac{C_1}{C}\right)^{n_m}\right)} \quad (1)$$

where n_m is described as the binding number of PS molecule per PMIPs and PNIPs site, D_m is the density of the receptor sites of the two employed adsorbents, and C_1 is the half-saturation concentration of the sorbed layer.

3.2. Sorption with the creation of two layers (M2)

This model suggested that the PS sorption on the PMIPs and PNIPs occurred by a fixed number of layers. Two layers are assumed in this state. The main active sites for the PS sorption can adsorb a non-fixed number of template molecules. This theoretical model considered two binding energies ($-\varepsilon_1$) and ($-\varepsilon_2$) that are associated with PS-PMIPs/PNIPs PMIPs and PNIPs, and PS-PS interactions. The equation of this model is obtained by (Wjiji et al., 2017):

$$Q_a = n_m D_m \frac{\left(\frac{C_1}{C}\right)^{n_m} + 2\left(\frac{C_2}{C}\right)^{2n_m}}{1 + \left(\frac{C_1}{C}\right)^{n_m} + \left(\frac{C_2}{C}\right)^{2n_m}} \quad (2)$$

where C_1 and C_2 are described as two concentrations at half-saturation that are associated with the 1st and 2nd adsorbed layers, and D_m is the receptor site density.

3.3. Sorption with a variable number of layers (M3)

This advanced model hypothesized that the PS sorption was performed with a non-fixed number of layers ($N_2 + 1$), and every binding site also captures a variable number of PS molecules. Two binding energies are examined to interpret the adsorption process: the first energy characterizes the interactions between the template molecules and the adsorbent surface and is mainly associated to the first layer (PS- PMIPs and PNIPs), and the second energy is associated to the interactions between PS molecules (PS-PS) (where N_2 is non-fixed). Therefore, the global number of layers is $(1 + N_2)$ and the expression of this adsorption model is obtained by the following equation (Yahia et al., 2019):

$$Q_a = n_m \cdot D_m \frac{-\frac{2\left(\frac{C_1}{C}\right)^{2n_m}}{\left(1 - \left(\frac{C_1}{C}\right)^{n_m}\right)} + \frac{\left(\frac{C_1}{C}\right)^{n_m} \left(1 - \left(\frac{C_1}{C}\right)^{2n_m}\right)}{\left(1 - \left(\frac{C_1}{C}\right)^{n_m}\right)^2} + \frac{2\left(\frac{C_1}{C}\right)^{n_m} \left(\frac{C_2}{C}\right)^{n_m} \left(1 - \left(\frac{C_2}{C}\right)^{n_m N_2}\right)}{\left(1 - \left(\frac{C_2}{C}\right)^{n_m}\right)} + \frac{\left(\frac{C_1}{C}\right)^{n_m} \left(\frac{C_2}{C}\right)^{n_m} \left(\frac{C_2}{C}\right)^{n_m N_2} N_2}{\left(1 - \left(\frac{C_2}{C}\right)^{n_m}\right)} + \frac{\left(\frac{C_1}{C}\right)^{n_m} \left(\frac{C_2}{C}\right)^{2n_m} \left(1 - \left(\frac{C_2}{C}\right)^{n_m N_2}\right)}{\left(1 - \left(\frac{C_2}{C}\right)^{n_m}\right)^2}}{\frac{\left(1 - \left(\frac{C_1}{C}\right)^{2n_m}\right)}{\left(1 - \left(\frac{C_1}{C}\right)^{n_m}\right)} + \frac{\left(\frac{C_1}{C}\right)^{n_m} \left(\frac{C_2}{C}\right)^{n_m} \left(1 - \left(\frac{C_2}{C}\right)^{n_m N_2}\right)}{\left(1 - \left(\frac{C_2}{C}\right)^{n_m}\right)}} \quad (3)$$

where C_1 and C_2 are the concentration at half-saturation of the first and $(N_2 + 1)$ PS sorbed layers on the two adsorbents. The expressions of the two adsorption energies are written as:

$$\Delta E_1 = RT \ln \frac{C_s}{C_1} \quad (4)$$

$$\Delta E_2 = RT \ln \frac{C_s}{C_2} \quad (5)$$

where C_s (mg/mL) is the PS water solubility, R is the ideal gas constant ($R = 8.314472 \text{ J}/(\text{mol}\cdot\text{K})$) and T is the absolute temperature.

4. Results and discussion

4.1. Simulation

These statistical physics adsorption models described in the previous section were adjusted to the equilibrium adsorption data at different operating temperatures. Three merits were utilized to select the adequate model using Origin 8 software. The first is the coefficient of determination (R^2) which defines the smallest sum of the squares of the residuals between the experimental and modeling data. The second is the akaike information criterion (AIC) and the third is the residual mean square error (RMSE) coefficient that can calculate the standard regression defect between the experimental data and the adjust model. In this regard, if the selected sorption model is suitable and the estimated parameters are unbiased, then approximately 95% of the estimated values should fall within ± 2 RMSE of their true values. The standard error determined by RMSE is written as (Alyousef et al., 2020):

$$\text{RMSE} = \sqrt{\frac{\text{RSS}}{m' - p}} \quad (6)$$

where RSS represents the sum of the residual squares, p is an adjustable parameter and m' expresses the number of the experimental data points.

Then, the relative quality estimator of the statistical physics models for a given data set AIC is defined as (Alyousef et al., 2020):

$$\text{AIC} = k \ln \left(\frac{\text{RSS}}{k} \right) + 2p \quad (7)$$

where k represents the number of experimental data points of the adsorption isotherm.

The total values of R^2 , RMSE and AIC coefficients of all the established models, as fitted to the adsorption isotherm

of PS on PMIPs and PNIPs, are summarized in Table 1. As can be noticed, the multilayer adsorption model provides the good adjusting results since it has the highest R^2 values and the lowest RMSE and AIC values in comparison with the

Table 1 Values of coefficient of determination R^2 , RMSE and AIC of each model.

Adsorbent	T(K)	Model		
		M1	M2	M3
R²				
Plate@MWCNT@MIPs	293	0.963	0.982	0.990
	303	0.962	0.981	0.994
	313	0.968	0.976	0.993
Plate@MWCNT@NIPs	293	0.964	0.983	0.992
	303	0.966	0.989	0.998
	313	0.968	0.986	0.991
RMSE				
Plate@MWCNT@MIPs	293	0.192	0.065	0.009
	303	0.162	0.092	0.003
	313	0.134	0.099	0.008
Plate@MWCNT@NIPs	293	0.171	0.053	0.004
	303	0.105	0.085	0.002
	313	0.114	0.052	0.007
AIC				
Plate@MWCNT@MIPs	293	14.25	4.23	2.16
	303	12.21	6.18	1.67
	313	10.33	7.34	2.05
Plate@MWCNT@NIPs	293	12.81	3.54	1.82
	303	9.15	5.86	1.22
	313	10.13	3.12	2.01

Table 2 Parameters values of the statistical physics (M3) for the adsorption of PS on PMIPs and PNIPs adsorbents.

Adsorbent	T (K)	Parameters					
		n_m	$D_m(\text{mg/g})$	N_c	$Q_{\text{asat}}(\text{mg/g})$	$\Delta E_1 (\text{kJ/mol})$	$\Delta E_2 (\text{kJ/mol})$
Plate@MWCNT@MIPs	293	2.46	1.15	4.82	13.63	6.36	4.56
	303	2.33	2.24	3.80	19.83	7.19	4.69
	313	2.26	3.62	3.35	27.40	7.62	4.79
Plate@MWCNT@NIPs	293	1.32	1.07	5.68	8.02	6.25	4.51
	303	1.21	1.97	4.64	10.98	7.08	4.57
	313	1.12	2.89	4.24	13.72	7.41	4.43

other applied models. Therefore, it was selected for the analysis and discussion of adsorption process. The adjusting of the sorption isotherms of prednisone on PMIPs and PNIPs according to the perfect-fitting model (M3) is illustrated in Fig. 2 and the different simulated parameters obtained from M3 are shown in Table 2. In the next section, the discussion of the fitted values of the adjusting parameters is interpreted, using a graphical representation of the behaviors as a function of temperature.

4.2. Steric interpretations

4.2.1. Study of the number of PS molecules linked per main adsorption site (n_m) and the density of receptor sites (D_m)

The parameter n_m involved in the saturated multilayer model can give a steric description concerning the PS molecules and the sorption process on the two tested adsorbents. This stoichiometric coefficient is also able to estimate the aggregation degree of PS (Bouaziz et al., 2019). In other words, this coefficient can provide a useful indication about the anchorage orientation of the PS molecule on the PMIPs and PNIPs

adsorbents by comparing its values to the unity. Microscopically, this parameter is in principle an integer or a fractional value for one site but the fitted number usually does not, because it expresses a mean value of the sites. Therefore, it can be lower or higher than unity. An n_m value superior to 1 expresses the anchored number of molecules per site, in accordance with a multi-molecular adsorption phenomenon (Bouaziz et al., 2019). An n_m value inferior to 1, expresses the portion of molecule per binding site if a multi-linking sorption phenomenon can be supposed. The calculated values of the n_m coefficient are represented in Table 2. As it can be shown, all the calculated n_m values for the PS adsorption on the two adsorbents at each operating temperature are greater than unity. This result indicates a non-parallel position for the adsorption of the PS molecules on both adsorbents. The PS molecules could link with one adsorption site where the adsorption is a multi-molecular process. For PS adsorbed on PMIPs, n_m is greater than 1, i.e. up to a value of 2.46. Since n_m is a mean number, we can assume that the effective number of binding of a PS molecule is either two or three, being one of the most frequent values. The precise proportion \times of sites

with two molecules corresponding to the $(1-x)$ proportion of sites bonding three molecules given by the following relation: $2.x + (1-x)0.3 = 2.46$. This would give 54% of the PS molecules doubly anchored at a single site, and 46% triply anchored at a single site. As depicted in Table 2, the n_m values varied from 2.26 to 2.46 and from 1.12 to 1.32 for the PS-PMIPs and PS-PNIPs sorption systems, respectively. Based on the estimated values of n_m , it has been observed that the aggregation degree is low i.e. the PS molecules only form a dimer ($n_m \approx 2$) for the first system and monomer ($n_m \approx 1$) for the second one at the three different temperatures. We can deduce that the adsorption system is not highly thermally activated. In other words, the temperature has a minor impact on the aggregation phenomenon. Comparatively, the number of PS molecules adsorbed by the main adsorbent site follows the next ranking: $n_m(\text{PS-PMIPs}) > n_m(\text{PS-PNIPs})$ at all operating temperatures. Chemically speaking, this trend can be explained by the textural properties of the adsorbents surface. It is clear that the PMIPs adsorbent is more attractive to the PS molecules than the PNIPs adsorbent. The impact of temperature on this coefficient is elucidated in Fig. 3 where the results show that the captured number n_m of PS molecules decreases with the increasing temperature. This fact is classically caused by the thermal agitation that generates the breakage of the binding between the adsorbed molecules in aqueous solution (Wjiji et al., 2017). So n_m is decreased with temperature as illustrated in Fig. 3.

Fig. 4 depicts the impact of the sorption temperature on the coefficient D_m , which is the density of the filled receptor sites per surface unit when they attain the saturation level. From this figure, it is noticed that this parameter presented an inverse behavior with respect to the n_m parameter. A decrease of n_m with temperature led to an increase of the parameter D_m , and vice versa. Firstly, the increase of temperature can lead, by a thermal dilatation, to an increase of the adsorption surface and the space on the PMIPs and PNIPs adsorbents surface. Secondly and particularly, an increase of the occupied binding sites, which could result from the decrease of n_m , causes the decrease of a steric hindrance effect. The size of the aggregated molecules before linkage and adsorption becomes small and other sites could be involved.

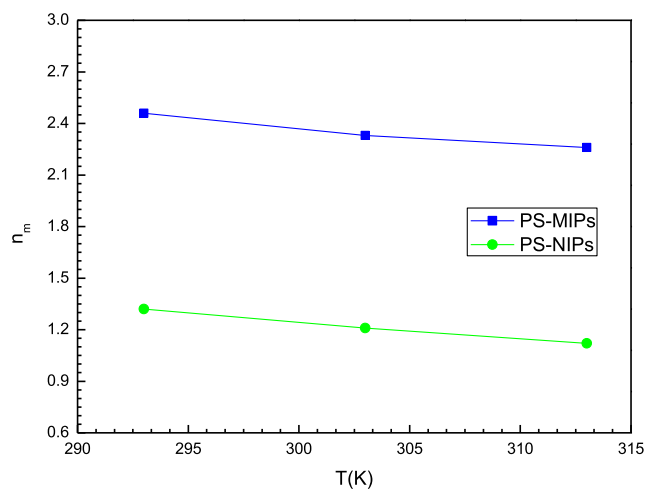


Fig. 3 Effect of temperature on the number n_m of PS molecules captured (from M3 model) onto PMIPs and PNIPs adsorbents.

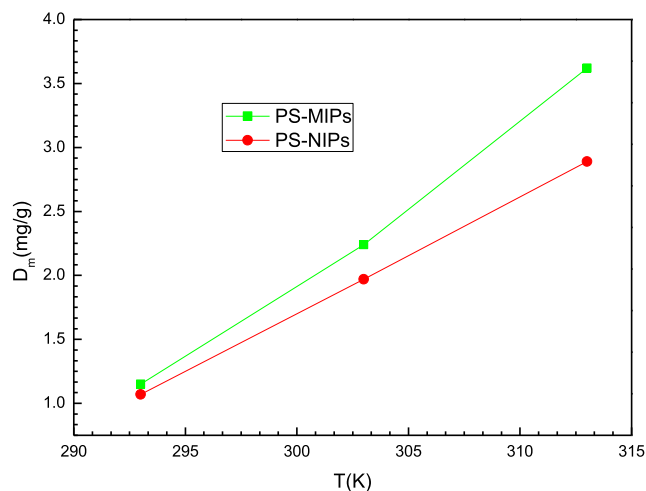


Fig. 4 Effect of temperature on the density of receptor sites (from M3 model) of MIPs and NIPs adsorbents.

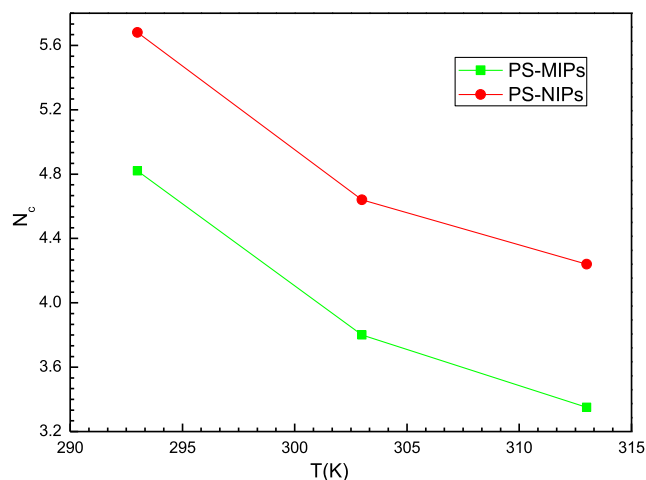


Fig. 5 Effect of temperature on the total number of formed layers of prednisone molecules (from M3 model) onto PMIPs and PNIPs adsorbents.

4.2.2. Study of the global number of adsorbed layers ($N_c = 1 + N_2$)

Fig. 5 depicts the impact of temperature on the overall number of formed layers of prednisone molecules on the PMIPs and PNIPs adsorbents. It was noticed that the temperature reduced the formation of the adsorbed layers for both adsorbents. It is therefore a classic thermal agitation effect. It was also shown (Table 2) that the sorbed layers varied from 4.82 to 3.35 and from 5.68 to 4.24 with temperature for the PS-PMIPs and PS-PNIPs systems, respectively. Four layers of PS molecules were arranged on the PMIPs surface at low temperature, and almost five layers of this template molecule (PS) were stacked on the surface of PNIPs. This difference is due to the textural and chemical properties of the two tested adsorbents surface, which affect the PMIPs/PNIPs-PS interactions and, therefore, the creation of the prednisone layers, such adsorption energies ($-\epsilon_1$), ($-\epsilon_2$) and cohesion energy between adsorbates molecules.

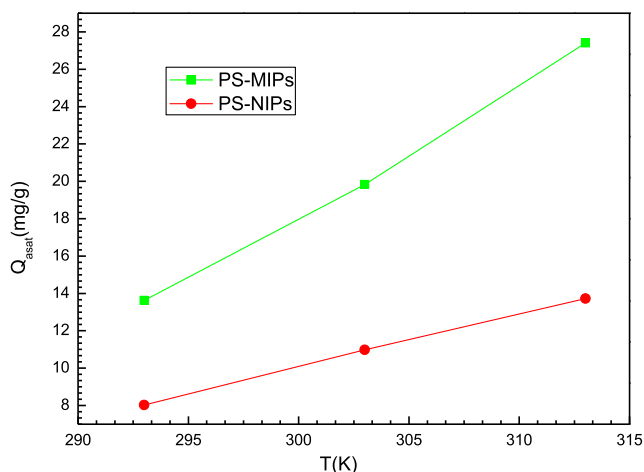


Fig.6 Effect of temperature on prednisone adsorption capacity at saturation (from M3 model) of PMIPs and PNIPs adsorbents.

4.2.3. Study of the prednisone uptake capacity at saturation

According to the saturated multilayer model, the adsorbed amount at saturation, $Q_{asat} = n_{ms} \cdot D_{sr} \cdot N_c$ is a steric coefficient related to the global number of sorbed layers, the density of receptor sites and the number of molecules per site. It represents the potentiality of the surface of the employed adsorbents to retain the PS molecules. The relationship between Q_{asat} and the tested temperature is illustrated in Fig. 6. It can be observed that the adsorbed amount at saturation of the two systems increased with the increasing temperature. This could be attributed to the important increase of D_m with temperature despite of the less important decrease of n_m and N_c with temperature. This behavior is not frequently observed and it may be explained using the steric coefficients (n_m , D_m and N_c) correlation. As aforementioned, the increase of temperature led to a decrease of the parameters n_m and N_c and to an increase of the parameter D_m . The trend of the three steric coefficients led to the rise of the uptake capacities with the temperature. Therefore, the parameter D_m is the main contributor to the evolution of the uptake capacities and has imposed the overall behavior. In terms of the performance of PS-PMIPs and PS-PNIPs, it was concluded that: Q_{asat} (PS-PMIPs) > Q_{asat} (PS-PNIPs). This ranking suggests that the PMIPs adsorbent is more effective to sorb the PS molecules. This is mainly due to the role of the surface of the PMIPs adsorbent, which can rapidly attract the amount of these target molecules, referring to the adjusted values of the adsorption parameters (n_m , D_m , and N_c) and adsorption energies. This can also be elucidated by the fact that the PS molecules can quickly recognize the imprinted sites and reduce the time of adsorption since the majority of the identification sites are presented on the polymers surface. Moreover, the template molecules (PS) were imprinted on the polymers surface during the formation of the PMIPs. After elimination of the template molecules, the spatial distribution, the size and the adsorption sites of imprinted pores were formed in the PMIPs adsorbent. However, the PNIPs material is prepared without the addition of a prednisone template. So prednisone cannot easily penetrate the target molecule cavity in the PNIPs during sorption, due to the difficulty of recognizing the main binding sites. This may explain its lower adsorption capacity compared to the PMIPs adsorbents.

4.3. Energetic interpretations and adsorption energies

The adsorption energy estimation is useful to obtain a suitable analysis of the adsorption phenomenon of PS on both adsorbents. The selected model provided two adsorption energies (Eqs. (4) and (5)) that were associated with the interactions between the prednisone molecules and between the prednisone and the sorbent surface. The adsorption energies were calculated and illustrated in Table 2. Note that the adsorption of PS on the tested adsorbent involved relatively weak adsorption interactions, which can be related to a physisorption process. Physical adsorption like hydrogen bonding usually presents values lower than 30 kJ mol^{-1} (Von Oepen et al., 1991). There are many other physisorption phenomena such as the hydrophobic binding forces of about 5 kJ mol^{-1} , the Van der Waals interactions generally of the order of 10 kJ mol^{-1} , the coordination exchanges of around 40 kJ mol^{-1} and the dipole bonding forces in the range $2\text{--}29 \text{ kJ mol}^{-1}$ (Cerofolini, 1974). In this work, the calculated adsorption energy (ΔE_1 and ΔE_2) values are inferior to 8 kJ mol^{-1} (Table 2) and consistent with the hydrophobic binding forces and the Van Der Waals interactions for the two adsorbents.

4.4. Site energy distribution

In order to estimate the site energy distribution, the Cerofolini approximation (Couture and Zitoun, 1992; Kumar et al., 2010; Kumar et al., 2011) was employed, in which the adsorption energy (ϵ) is associated to the equilibrium concentration (C) of the adsorbate, and can be written as:

$$C = C_s e^{\frac{\epsilon}{kT}} \quad (8)$$

By substituting Eq. (7) into Eq. (3), the isotherm $Q_a(c)$ can be obtained as a function of ϵ , and expressed as $Q_a(\epsilon)$. Then, by differentiating the isotherm $Q_a(\epsilon)$ with respect to ϵ , the distribution of site energy $F(\epsilon)$ is given as follows:

$$F(\epsilon) = \frac{dQ_a}{d\epsilon} \quad (9)$$

Fig. 7 illustrates three adsorption energy distributions (AEDs) according to Eq. (9) for the sorption of PS at three operating temperatures on the PMIPs and PNIPs adsorbents. It was seen that the two tested adsorbents show a unimodal distribution of approximately Gaussian type binding sites. It was also observed that all the curves have the same shapes and the same normal distribution but different intensities of energy associated with the maximum peak. In addition, it can be seen that the maximum peak height decreases gradually with respect to temperature. As can be observed, the distribution of energy for both adsorbents systems appears to evolve towards higher energy values with a rising temperature. This indicates that the binding sites with low adsorption energy are becoming less accessible for prednisone sorption. These sorption energies mainly spread in broad peaks, centered on values relatively close to the sorption energies adjusted by the adopted model. Indeed, the energy distribution graph spans along the abscissa axis by displaying a single peak for well-defined energy values which most probably describes the means of the sorption energies of the entire distribution. This can be explained by the fact that, in a solution at a tested temperature, the prednisone molecules, agitated by the movement

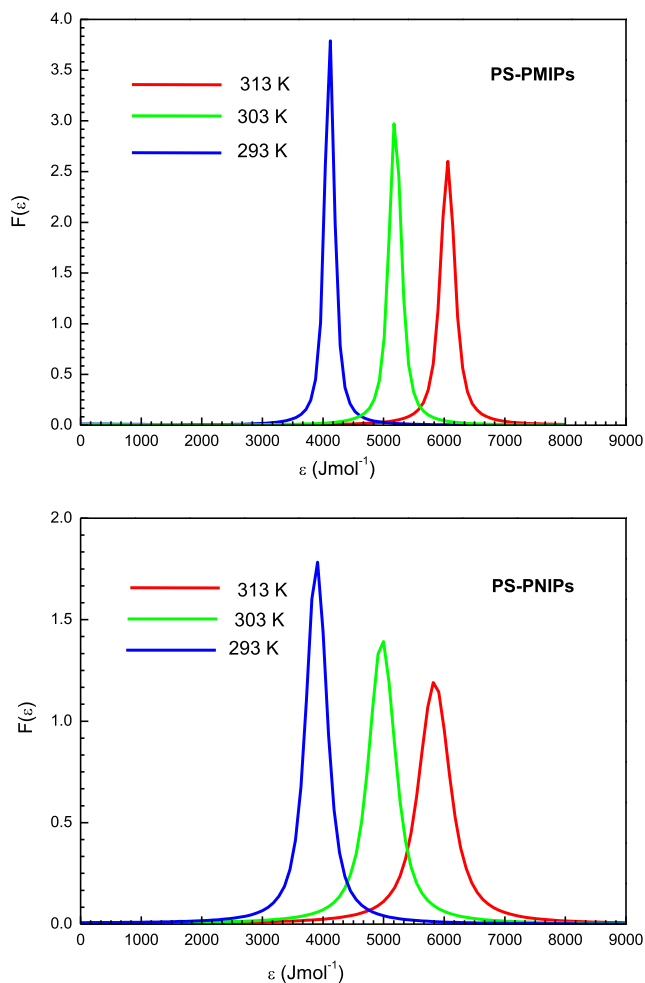


Fig. 7 Site energy distributions of PS adsorption onto PMIPs and PNIPs adsorbents.

of thermal agitation, are provided with a kinetic energy proportional to the solution temperature: the higher the temperature, the higher the mean particle velocity. Thus, we can observe that during the rise of the temperature, the binding sites should have higher sorption energy to capture the target molecules, and the lower energy sites cannot anymore capture the PS molecules. This observation indicates that both adsorbents have more than one energy state for the uptake of prednisone molecules within the tested concentration range. Consequently, PMIPs and PNIPs have heterogeneous surfaces, and the differences in the maximum peaks are due to the temperature variation. Comparatively, the intensity of energy of PMIPs is relatively higher than that of PNIPs, thus corroborating the differences of the structure in these recognition materials. It is observed that the adsorption energy values are limited to 7 kJ/mol, which affirms that this is indeed a physisorption.

4.5. Thermodynamic function

The adsorption multilayer model with saturation is used to estimate some fundamental thermodynamic potential functions, like internal energy (E_{int}), Gibbs free energy (G) and adsorption entropy (S). These three functions can contribute

in the macroscopic analysis of the prednisone adsorption on the PMIPs and PNIPs adsorbents, as interpreted in the subsequent.

4.5.1. Internal energy analysis

Generally, the internal energy formulation can be obtained using the grand canonical partition function of our best fitting model, in order to thermodynamically analyze the PS adsorption mechanism. The formula of the internal energy is represented by the following equation [48]:

$$E_{\text{int}} = -\frac{\partial \ln Z_{\text{gc}}}{\partial \beta} + \frac{\mu}{\beta} \left(\frac{\partial \ln Z_{\text{gc}}}{\partial \mu} \right) \quad (10)$$

where β is formulated as $1/k_{\text{B}}T$, with k_{B} is the constant of Boltzmann and T is the absolute temperature, and μ is the chemical potential.

The variation of the internal energy (E_{int}) at three operating temperatures is depicted in the Fig. 8. From this figure, it is observed that the values of internal energy (E_{int}) are negative for the three tested temperatures. This affirms that the two adsorbent systems vary spontaneously, as they release energy. Additionally, the module of the internal energy (E_{int}) values

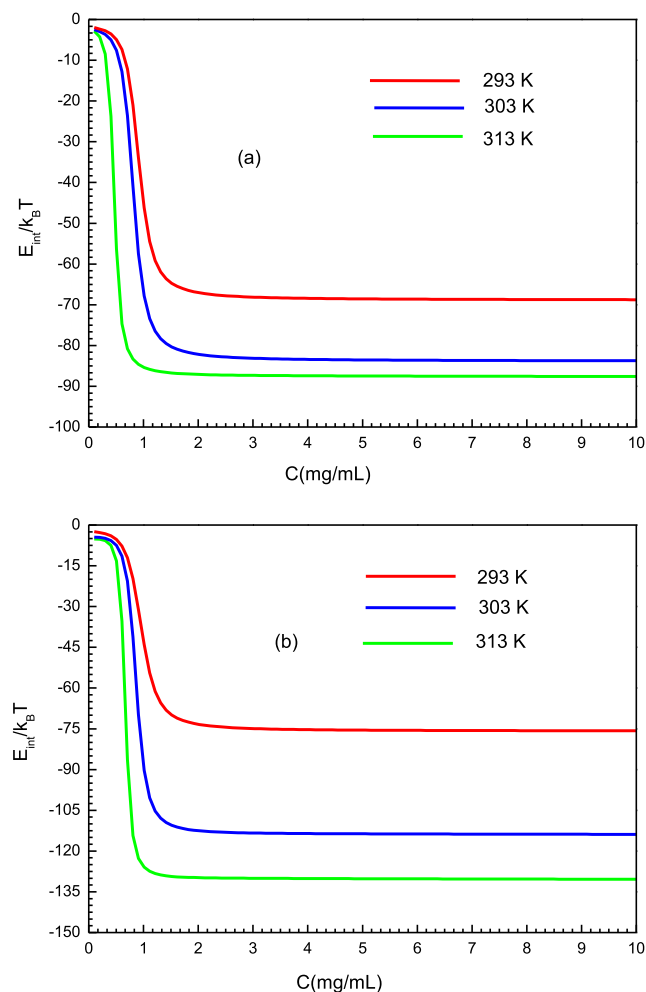


Fig. 8 Variation of the internal energy according to the concentration for the two tested adsorption system (a) of PMIPs and (b) PNIPs at different temperature.

rises with an increment of temperature. This can be elucidated by the growth of the interaction between the PS molecules and the surface of the molecular recognition materials (PMIPs and PNIPs), also associated with the increase in the thermal collisions of PS molecules with the sorbent surface. Thus, when the molecule of PS is coordinated to the main binding site of PMIPs/PNIPs adsorbents surface, it needs to release energy.

4.5.2. Free enthalpy analysis

The free enthalpy is a thermodynamic function which can be used to characterize and to corroborate the sorption mechanism spontaneity involved in the tested systems. It can be derived by this equation [48]:

$$G = \mu Q_a \quad (11)$$

where Q_a expresses the uptake capacity.

The variation of the free enthalpy at three operating temperatures is depicted in Fig. 9. According to this figure, it can be concluded that, at a quiet value of concentration, G undergoes a rapid decrease with a raising concentration. Furthermore, the values of the free enthalpy are negative, demonstrating that the PS sorption on PMIPs/PNIPs varies in a

spontaneous thermodynamic way. Additionally, the absolute value of G rises with respect to temperature, which means that the adsorption feasibility involved in the PMIPs and PNIPs adsorbents raises at high temperatures.

4.5.3. Sorption entropy analysis

The sorption entropy (S) provides very important indications about the adsorption process. Particularly, it characterizes the disorder evolution of prednisone molecules adsorption onto PMIPs and PNIPs surfaces. The equation of this function (S) is represented by Kumar et al. (2010):

$$J = -k_B T \ln Z_{gc} \quad (12)$$

$$J = -\frac{\partial \ln Z_{gc}}{\partial \beta} - TS \quad (13)$$

From which the entropy expression can be obtained as follows:

$$\frac{S}{k_B} = -\beta \frac{\partial \ln Z_{gc}}{\partial \beta} + \ln Z_{gc} \quad (14)$$

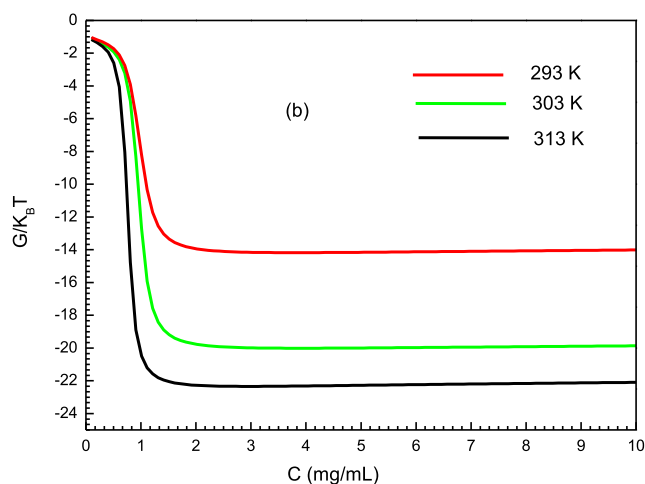
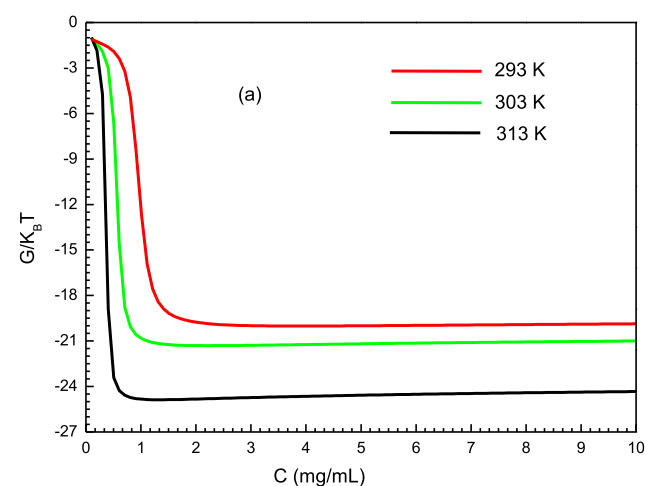


Fig. 9 Variation of the free enthalpy according to the concentration for the two studied adsorption system (a) of PMIPs and (b) PNIPs at different temperature.

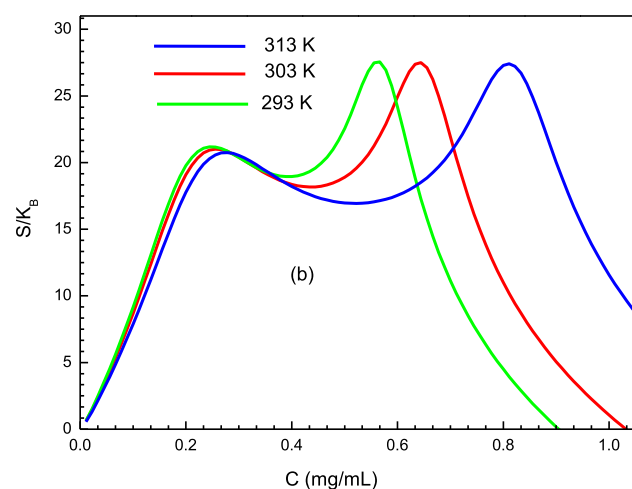
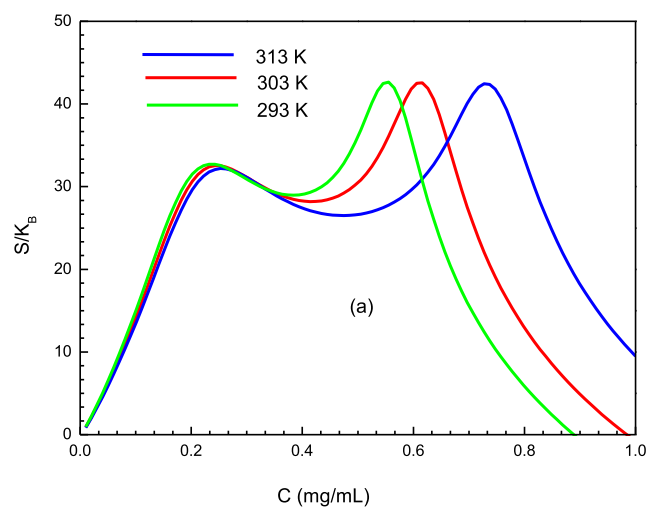


Fig. 10 Variation of the entropy according to the concentration for the two studied adsorption system (a) of PMIPs and (b) PNIPs at different temperature.

The variation of the adsorption entropy at three tested temperatures is depicted in Fig. 10. According to the adsorption entropy graph, we observe that the entropy has a similar shape at the three operating temperatures. Particularly, we notice that the behavior of the adsorption entropy shows two peaks related to the 1st and 2nd half-saturation concentration values, (C_1) and (C_2), respectively. In fact, at the start of the adsorption mechanism, we observe that the entropy values begin from a null value. Then the variation of entropy (S) attains a maximum value close to the first half-saturation concentration ($C \leq C_1$). This implies that the disorder is maximum ($C = C_1$) when half of the binding sites ($D_m/2$) of the 1st layer are filled. Afterwards, the entropy value diminishes when the total of the binding sites of the first layer are completely filled. In fact, if the concentration is lower than that of the half-saturation ($C \leq C_1$), the target molecule has many possibilities to link to an active site, to be captured, and consequently, the disorder rises to the surface with the sorption amount. Beyond the first half-saturation ($C \geq C_1$), the number of vacant binding sites of the 1st formed layer diminishes and the number of available states becomes rather limited. Therefore, the entropy values decrease since the probability of detecting vacant first-type sites decreases progressively when the saturation of the first formed layer is almost attained. However, it can be seen that the minimum entropy value does not attain zero, since before the first-layer sites are fully saturated, the N_2 layers begin to be occupied by the PS molecules and thus their sorption entropy tends to rise again. Then, the sorption entropy (S) continues the same trend around C_2 as that obtained around C_1 . Finally, the entropy values attain zero, when the saturation is fully reached and sorption is finished.

5. Conclusions

In this paper, the adsorption mechanism of PS on PMIPs and PNIPs adsorbents was theoretically investigated. The experimental PS adsorption isotherms at three operating temperatures were simulated and analyzed in light of the saturated multilayer model. This model is developed through a statistical physics formalism using the grand canonical ensemble. The modeling examination suggested that the PS adsorption process was related to the formation of around three of the four or five adsorbed layers depending on the adsorbent surfaces and temperature. The theoretical results indicated that the nonparallel adsorption positions of the PS on the two employed adsorbents are observable where the adsorption is a multi-molecular process. It was also reported that the PS molecules aggregated in solution and mainly formed a monomer for the first system (PMIPs) and a dimer for the second one (PNIPs). The variation of the uptake capacity at saturation could be explained by the endothermic phenomenon. According to the adsorption energy evaluation, physical interactions can be involved in the PS adsorption phenomenon. A general analytical analysis of the modeling indicated that the receptor sites density is the main factor that governed the adsorption phenomenon. The investigation of the distribution of the adsorption energy (AED) indicated that the function of distribution represents an approximately Gaussian shape and asserted the physical nature of the PS adsorption phenomenon. A thermodynamic analysis demonstrated that the PS adsorption is energetically spontaneous

and releases energy for both systems and at different tested temperatures.

Declaration of Competing Interest

The authors declared that there is no conflict of interest.

Acknowledgments

The authors would like to thank the Center for Promising Research in Social Research and Women's Studies Deanship of Scientific Research, at Princess Nourah bint Abdulrahman University for funding this Project in 2020.

References

- Akram, K., Dorabei, R.Z., 2017. Ultrasound-assisted dispersive magnetic solid phase extraction for preconcentration and determination of trace amount of Hg (II) ions from food samples and aqueous solution by magnetic graphene oxide (Fe₃O₄@ GO/2-PTSC): central composite design optimization. *Ultrason. Sonochem.* 38, 421–429.
- Almughamisi, S.M., Khan, Z.A., Alshitari, W., Elwakeel, K.Z., 2020. Recovery of Chromium(VI) Oxyanions from Aqueous Solution Using Cu(OH)₂ and CuO Embedded Chitosan Adsorbents. *J. Polym. Environ.* 28, 47–60.
- Alyousef, H. et al, 2020. Statistical physics modeling of water vapor adsorption isotherm into kernels of dates: Experiments, microscopic interpretation and thermodynamic functions evaluation. *Arab. J. Chem.* 13, 4691–4702.
- Anderson, R.A., Ariffin, M.M., Cormack, P.A.G., Miller, E.I., 2008. Comparison of molecularly imprinted solid-phase extraction (MISPE) with classical solid-phase extraction (SPE) for the detection of benzodiazepines in post-mortem hair samples. *Forensic Sci. Int.* 174, 40–46.
- Antignac, J.P., Monteau, F., Nègriolli, J., André, F., Le Bizec, B., 2004. Application of hyphenated mass spectrometric techniques to the determination of corticosteroid residues in biological matrices. *Chromatographia* 59, S13–S22.
- Aouaini, F., Bouzgarrou, S., Khemiri, N., Ben Yahia, M., Almogait, S.E., AlHarbi, F.F., Almuqrin, H.A., Ben Lamine, A., 2019. Study of the CO₂ adsorption isotherms on El Hicha clay by statistical physics treatment: microscopic and macroscopic investigation. *Sep. Sci. Technol.* 54, 2577–2588.
- Arabi, M., Ostovan, A., Bagheri, A.R., Guo, X., Wang, L., Li, J., Wang, X., Li, B., Chen, L., 2020. Strategies of molecular imprinting-based solid-phase extraction prior to chromatographic analysis. *TrAC, Trends Anal. Chem.* 128, 1–98.
- Bagot, R.C., Meaney, M.J., 2011. Separation of steroids and the determination of estradiol content in transdermic patches by microemulsion electrokinetic chromatography. *Chromatographia* 73, 373–378.
- Bianchi, V.D.N., Silva, M.R.D., Lamim, M.A., Silva, C.L.D., Lima, E.C.D., 2017. Solid phase extraction using molecular imprinting polymers (MISPE) for the determination of estrogens in surface water by HPLC. *Rev. Ambient. Água.* 12, 381–289.
- Bouaziz, N., Ben Torkia, Y., Aouaini, F., Nakbi, A., Dhaou, H., Ben Lamine, A., 2019. Statistical physics modeling of hydrogen absorption onto LaNi_{4.6}Al_{0.4}: Stereographic and energetic interpretations. *Sep. Sci. Technol.* 54, 2589–2608.
- Bouaziz, N., Ben Manaa, M., Aouaini, F., Ben Lamine, A., 2019. Investigation of hydrogen adsorption on zeolites A, X and Y using statistical physics formalism 225, 111–121.
- Capelli, A.M., Bruno, A., Guadix, A.E., Costantino, G., 2013. Unbinding pathways from the glucocorticoid receptor shed light on the reduced sensitivity of glucocorticoid ligands to a naturally

- occurring, clinically relevant mutant receptor. *J. Med. Chem.* 56, 7003–7014.
- Cerofolini, G.F., 1974. Localized adsorption on heterogeneous surfaces. *Thin Solid Films* 23, 129–152.
- Couture, L., Zitoun, R., 1992. *Physique statistique. Ellipses, Paris.*
- Elwakeel, K.Z., Shahat, A., Al-Bogami, A.S., Wijesiri, B., Goonetilleke, A., 2020. The synergistic effect of ultrasound power and magnetite incorporation on the sorption/desorption behavior of Cr (VI) and As(V) oxoanions in an aqueous system. *J. Colloid. Interf. Sci.* 569, 76–88.
- Ertan, B., Eren, T., Ermiş, I., Saral, H., Atar, N., Yola, M.L., 2016. Recent Sensitive analysis of simazine based on platinum nanoparticles on polyoxometalate/multi-walled carbon nanotubes. *J. Colloid Interface Sci.* 470, 14–21.
- Fiori, J., Andrisano, V., 2014. method for the simultaneous determination of six glucocorticoids in pharmaceutical formulations and counterfeit cosmetic products. *J. Pharm. Biomed. Anal.* 91, 185–192.
- Fu, Q., Shou, M., Chien, D., Markovich, R., Rustum, A.M., 2010. Development and validation of a stability-indicating RP-HPLC method for assay of betamethasone and estimation of its related compounds. *J. Pharm. Biomed. Anal.* 51, 617–625.
- Gagliardi, L., De Orsi, D., Manna, F., Tonelli, D., 2000. HPLC determination of clobetasol propionate in cosmetic products. *J. Liq. Chromatogr. Relat. Technol.* 23, 355–362.
- Gagliardi, L., De Orsi, D., Del Giudice, M.R., Gatta, F., Porra, R., Chimenti, P., Tonelli, D., 2002. Development of a tandem thin-layer chromatography-high-performance liquid chromatography method for the identification and determination of corticosteroids in cosmetic products. *Anal. Chim. Acta* 457, 187–198.
- Gong, H., Hajizadeh, S., Ye, L., 2018. Dynamic assembly of molecularly imprinted polymer nanoparticles. *J. Colloid Interface Sci.* 509, 463–471.
- Kamra, T., Chaudhary, S., Xu, C., Johansson, N., Montelius, L., Schnadt, J., Ye, L., 2015. Covalent immobilization of molecularly imprinted polymer nanoparticles using an epoxy silane. *J. Colloid Interface Sci.* 445, 277–284.
- Kumar, K.V., de Castro, M.M., Martinez-Escandell, M., Molina-Sabio, M., Silvestre-Albero, J., Rodriguez Reinoso, F., 2010. A continuous site energy distribution function from Redlich-Peterson isotherm for adsorption on heterogeneous surfaces. *Chem. Phys. Lett.* 492, 187–192.
- Kumar, D.R., Manoj, D., Santhanalakshmi, J., 2014. Optimization of oleylamine-Fe₃O₄/MWCNTs nanocomposite modified GC electrode for electrochemical determination of ofloxacin. *J. Nanosci. Nanotechnol.* 14, 5059–5069.
- Kumar, K.V., Serrano-Ruiz, J.C., Souza, H.K.S., Silvestre-Albero, A.M., Gupta, V.K., 2011. Site energy distribution function for the sips isotherm by the condensation approximation method and its application to characterization of porous materials. *J. Chem. Eng. Data* 56, 2218–2224.
- Li, M., Jin, M.M., Chen, X., Shao-ming, S., Juan, L., 2013. Determination of 3 corticosteroids in cosmetics by field amplified sample introduction-micellar capillary electrophoresis. *Phys. Test Chem. Anal. Part B: Chem. Anal.* 49, 435–438.
- Liu, Y., Cao, B., Jia, P., An, J., Luo, C., Ma, L., Chang, J., Pan, K., 2015. Layer-by-layer surface molecular imprinting on polyacrylonitrile nanofiber mats. *J. Phys. Chem. A* 119, 6661–6667.
- Liu, M., Li, X., Li, J., Wu, Z., Wang, F., Liu, L., Tan, X., Lei, F., 2017. Selective separation and determination of glucocorticoids in cosmetics using dual-template magnetic molecularly imprinted polymers and HPLC. *J. Colloid Interface Sci.* 504, 124–133.
- Luo, Y.B., Yu, Q.W., Yuan, B.F., Feng, Y.Q., 2012. Fast microextraction of phthalate acid esters from beverage, environmental water and perfume samples by magnetic multiwalled carbon nanotubes. *Talanta* 90, 123–131.
- Nematollahzadeh, A., Shojaei, A., Abdekhodaie, M.J., Sellergren, B., 2014. Molecularly imprinted polydopamine nano-layer on the pore surface of porous particles for protein capture in HPLC column. *J. Colloid Interface Sci.* 51, 261–267.
- Reepmeyer, J.C., Revelle, L.K., Vidavsky, I., 1998. Detection of clobetasol propionate as an undeclared steroid in zinc pyrithione formulations by high-performance liquid chromatography with rapid-scanning ultraviolet spectroscopy and mass spectrometry. *J. Chromatogr. A* 828, 239–246.
- Rodionova, O., Pomerantsev, A., Houmøller, L., Shpak, A., Shpigun, O., 2010. Noninvasive detection of counterfeited ampoules of dexamethasone using NIR with confirmation by HPLC-DAD-MS and CE-UV methods. *Anal. Bioanal. Chem.* 397, 1927–1935.
- Santoni, O., 2015. *EU Cosmetics Regulation, Workshop on Natural Cosmetics*. University of Bangor, p. 2.
- Song, X., Niu, Y., Qiu, Z., Zhang, Z., Zhou, Y., Zhao, J., Chen, H., 2017. Adsorption of Hg(II) and Ag(I) from fuel ethanol by silica gel supported sulfur-containing PAMAM dendrimers: Kinetics, equilibrium and thermodynamics. *Fuel* 206, 80–88.
- Song, X., Niu, Y., Zhang, P., Zhang, C., Zhang, Z., Zhu, Y., Qu, R., 2017. Removal of Co(II) from fuel ethanol by silica-gel supported PAMAM dendrimers: combined experimental and theoretical study. *Fuel* 199, 91–101.
- Von Oepen, B., Kördel, W., Klein, W., 1991. Sorption of nonpolar and polar compounds to soils: processes, measurements and experience with the applicability of the modified OECD-guideline 106. *Chemosphere* 22, 285–304.
- Wang, F., Li, X., Li, J., Zhu, C., Liu, M., Wu, Z., Liu, L., Tan, X., Lei, F., 2018. Preparation and application of a molecular capture for safety detection of cosmetics based on surface imprinting and multi-walled carbon nanotubes. *J. Colloid Interface Sci.* 527, 124–131.
- Wei, L., Yan, S., Yang, C., Yan, X., Guo, H., Fu, G., 2015. Fabrication of surface protein-imprinted nanoparticles using a metal chelating monomer via aqueous precipitation polymerization. *ACS Appl. Mater. Interfaces* 7, 27188–27196.
- Wjihi, S., Erto, A., Knani, S., Lamine, A.B., 2017. Investigation of adsorption process of benzene and toluene on activated carbon by means of grand canonical ensemble. *J. Mol. Liq.* 238, 402–410.
- Yahia, B. et al, 2019. Adsorption of sodium and lithium ions onto helicenes molecules: Experiments and phenomenological modeling. *J. Mol. Liq.* 288, 110998.
- Zhang, Z., Hu, Y., Zhang, H., Yao, S., 2010. Novel layer-by-layer assembly molecularly imprinted sol-gel sensor for selective recognition of clindamycin based on Au electrode decorated by multi-wall carbon nanotube. *J. Colloid Interface Sci.* 344, 158–164.
- Zhang, J., Li, Z., Zhou, Z., Bai, Y., Liu, H., 2016. Rapid screening and quantification of glucocorticoids in essential oils using direct analysis in real time mass spectrometry. *Rapid Commun. Mass Spectrom.* 30, 133–140.
- Zhang, Z., Niu, Y., Chen, H., Yang, Z., Bai, L., Xue, Z., Yang, H., 2019. Feasible one-pot sequential synthesis of aminopyridine functionalized magnetic Fe₃O₄ hybrids for robust capture of aqueous Hg(II) and Ag(I). *ACS Sustain. Chem. Eng.* 7, 7324–7337.
- Zhang, H.F., Shi, Y.P., 2012. Preparation of Fe₃O₄ nanoparticle enclosure hydroxylated multi-walled carbon nanotubes for the determination of aconitines in human serum samples. *Anal. Chim. Acta* 724, 54–60.
- Zhao, H., Liu, X., Cao, Z., Zhan, Y., Zhou, J., Xu, J., 2016. Adsorption behavior and mechanism of chloramphenicols, sulfonamides, and non-antibiotic pharmaceuticals on multi-walled carbon nanotubes. *J. Hazard. Mater.* 310, 235–245.
- Zhou, Y., Luan, L., Tang, B., Niu, Y., Qu, R., Liu, Y., Xu, W., 2020. Fabrication of Schiff base decorated PAMAM dendrimer/magnetic Fe₃O₄ for selective removal of aqueous Hg(II). *J. Chem. Eng.* 398, 125–651.
- Zong-Yuan, W., Xiao-Yan, L., Xiao-Meng, S., Min, L., 2014. Study of online molecularly imprinted solid phase extraction techniques in food safety analysis. *J. Food Saf. Qual.* 5, 1297–1304.